The Journal of Experimental Biology 216, 623-632

doi:10.1242/jeb.074401

RESEARCH ARTICLE

Mechanisms of transepithelial ammonia excretion and luminal alkalinization in the gut of an intestinal air-breathing fish, *Misgurnus anguilliacaudatus*

Jonathan M. Wilson[1,*], Joana Moreira-Silva[1,2], Inês L. S. Delgado[1], Sue C. Ebanks[3], Mathilakath M. Vijayan[4], João Coimbra[1,2] and Martin Grosell[3]

[1]Laboratório de Ecofisiologia, CIMAR/CIIMAR – Centro Interdisciplinar de Investigação Marinha e Ambiental – Universidade do Porto, Portugal, [2]Instituto de Ciências Biomédicas de Abel Salazar da Universidade do Porto, Portugal, [3]Rosenstiel School of Marine and Atmospheric Science/Division of Marine Biology and Fisheries, University of Miami, Miami, USA and [4]Department of Biology, University of Waterloo, Waterloo, ON, Canada

*Author for correspondence (wilson.jm.cimar@gmail.com)

SUMMARY

The weatherloach, *Misgurnus angulliacaudatus*, is an intestinal air-breathing, freshwater fish that has the unique ability to excrete ammonia through gut volatilization when branchial and cutaneous routes are compromised during high environmental ammonia or air exposure. We hypothesized that transepithelial gut NH_4^+ transport is facilitated by an apical Na^+/H^+ (NH_4^+) exchanger (NHE) and a basolateral $Na^+/K^+(NH_4^+)$-ATPase, and that gut boundary layer alkalinization ($NH_4^+ \rightarrow NH_3 + H^+$) is facilitated by apical HCO_3^- secretion through a Cl^-/HCO_3^- anion exchanger. This was tested using a pharmacological approach with anterior (digestive) and posterior (respiratory) intestine preparations mounted in pH-stat-equipped Ussing chambers. The anterior intestine had a markedly higher conductance, increased short-circuit current, and greater net base (J_{base}) and ammonia excretion rates (J_{amm}) than the posterior intestine. In the anterior intestine, HCO_3^- accounted for 70% of J_{base}. In the presence of an imposed serosal–mucosal ammonia gradient, inhibitors of both NHE (EIPA, 0.1 mmol l^{-1}) and Na^+/K^+-ATPase (ouabain, 0.1 mmol l^{-1}) significantly inhibited J_{amm} in the anterior intestine, although only EIPA had an effect in the posterior intestine. In addition, the anion exchange inhibitor DIDS significantly reduced J_{base} in the anterior intestine although only at a high dose (1 mmol l^{-1}). Carbonic anhydrase does not appear to be associated with gut alkalinization under these conditions as ethoxzolamide was without effect on J_{base}. Membrane fluidity of the posterior intestine was low, suggesting low permeability, which was also reflected in a lower mucosal–serosal J_{amm} in the presence of an imposed gradient, in contrast to that in the anterior intestine. To conclude, although the posterior intestine is highly modified for gas exchange, it is the anterior intestine that is the likely site of ammonia excretion and alkalinization leading to ammonia volatilization in the gut.

Supplementary material available online at http://jeb.biologists.org/cgi/content/full/216/4/623/DC1

Key words: ammonia volatilization, chloride–bicarbonate exchanger, sodium–proton exchanger, sodium–potassium ATPase, ammonium.

Received 26 April 2012; Accepted 8 October 2012

INTRODUCTION

The weatherloach (*Misgurnus anguillicaudatus*) is a non-obligate intestinal air-breathing freshwater fish (Graham, 1997; McMahon and Burggren, 1987). The gastrointestinal tract of the loach is highly modified for gas exchange, with the posterior intestine (two-thirds of the total gut length) lacking characteristic absorptive columnar enterocytes, and instead having a well-vascularized stratified epithelium with intraepithelial capillaries suitable for gas exchange (McMahon and Burggren, 1987; Gonçalves et al., 2007; Wilson and Castro, 2010). The loach accomplishes intestinal air-breathing by swallowing air and passing it down the length of the gut unidirectionally. The intestine is characteristically inflated with air even during feeding, with the intestinal fluid limited to a surface film (Jeuken, 1957; McMahon and Burggren, 1987). Tsui and colleagues (Tsui et al., 2002) provided evidence that the gut is the site of ammonia volatilization, the rate of which increases from 0.05 to 0.80 μmol total ammonia nitrogen (TAN) g^{-1} day^{-1} when branchial and cutaneous routes of ammonia excretion are compromised (>90%) by air exposure or high environmental ammonia (HEA) levels. The use of the gut as an accessory air-breathing organ for both oxygen uptake and ammonia excretion allows the loach to survive periods of drought and poor water quality (hypoxia, HEA) that characterize its natural environment.

Consequently, the weatherloach is a very ammonia-tolerant fish (Chew et al., 2001; Tsui et al., 2002; Moreira-Silva et al., 2010). Under ammonia-loading conditions (HEA or emersion), the accumulation of ammonia in the body together with the increase in blood pH will favor an outward gradient of ammonia (Tsui et al., 2002). This evidence would argue in favor of passive transepithelial NH_3 diffusion as the probable mechanism for ammonia excretion; however, alkalinization of the gut luminal surface from pH 7.4 up to pH 8.2 has also been observed (Tsui et al., 2002), which would be inconsistent with this mechanism as backflux of NH_3 would occur. Instead, we propose facilitated transport of NH_4^+ as the mechanism of ammonia excretion.

NH_4^+ has been shown to be transported by Na^+/H^+ exchangers (NHEs) and Na^+/K^+-ATPase by replacing H^+ and K^+, respectively (Knepper et al., 1989; Mallery, 1983; Randall et al., 1999). Both these transporters have been well characterized in the vertebrate intestine, with the basolateral Na^+/K^+-ATPase having an important

role in driving transepithelial transport processes (nutrient and ion regulation) (Grosell, 2010; Marshall and Grosell, 2006). In mammals, the intestinal NHEs are involved in intracellular pH regulation and Na^+ uptake (Zachos et al., 2005). The NHE isoform 1 (NHE1) is expressed at the basolateral membrane, whereas NHE2 is apical and NHE3 is recycled between intracellular vesicles and the plasma membrane (Zachos et al., 2005). Gut lumen surface alkalinization in the loach is probably accomplished through HCO_3^- excretion in exchange for Cl^- as has been reported in marine fishes (Grosell et al., 2009b). Although intestinal base excretion has been reported in freshwater trout (Genz et al., 2011), the mechanism of luminal alkalinizaton has only been well characterized in marine fishes, which imbibe water for osmoregulation (Grosell, 2006). The intestinal anion exchanger responsible for alkalinization in marine teleosts has been determined to be Slc26a6 (Kurita et al., 2008; Grosell et al., 2009b) although in freshwater trout gut expression is generally absent (Genz et al., 2011).

In the present study, the mechanisms of ammonia and base excretion in the weatherloach gut were characterized using a pharmacological approach. Investigation of the roles of Na^+/K^+-ATPase and NHE on NH_4^+ transport utilized the inhibitors ouabain and EIPA (see below), respectively, while the roles of the Cl^-/HCO_3^- anion exchanger and carbonic anhydrase (CA) in gut alkalinization were assessed using DIDS (see below) and ethoxzolamide, respectively. The electrophysiological properties of the different regions of the gut (anterior *versus* posterior intestine) and their membrane fluidity were also assessed.

MATERIALS AND METHODS

Animals

Adult weatherloaches, *M. anguillicaudatus* (Cantor 1842), were purchased from the main wet market in Yuen Long, Hong Kong, and maintained at the Department of Biology and Chemistry, City University, Hong Kong. Fish for Ussing chamber experiments were transported to the Rosenstiel School of Marine and Atmospheric Science, University of Miami, by air freight with minimal water. Upon arrival, fish were maintained in 10 l flow-through glass aquaria containing dechlorinated Virgina Key tap water (Na^+ 0.35 mmol l^{-1}, hardness 45 mg l^{-1} $CaCO_3$, pH 7.5), at 25°C, under natural light conditions. During this period the fish were fed daily *ad libitum* with commercial fish food (Granured, Sera GmbH, Germany), and the feed was withheld 48 h prior to the start of experimental procedures. Procedures were approved by the University of Miami Animal Care and Use Committee.

In vitro ammonia flux experiment

Weatherloaches (10.97±6.68 g and 11.2±1.6 cm, means ± s.d.) were treated with an overdose of neutralized tricane methanesulfonate [1:5000 (w/v), Syndel Lab, Qualicum Beach, BC, Canada] and killed by decapitation. The entire gut was excised, cut ventrally along its entire length and laid out over a paper towel moistened with artificial serosal saline (Table 1), for immediate mounting in the Ussing chamber system (P2300, Physiologic Instruments, San Diego, CA, USA).

Electrophysiology and pH-stat analysis

The anterior and the most posterior region of the intestine were mounted on tissue-holding cassettes [P2403 (0.1 cm^2) to P2413 (0.71 cm^2), depending on the size of the tissue; Physiologic Instruments]. The tissue inserts were mounted in Ussing chambers and both serosal and mucosal chambers were filled with 1.6 ml of pre-gassed serosal saline (see Table 1 for saline composition) maintained at 25°C. The saline solutions were continually gassed with 0.3% CO_2/O_2, to ensure the proper mixing of both half-chambers. Current and voltage electrodes were connected to an amplifier (VCC600, Physiologic Instruments), and data transferred to a PC using the BIOPAC systems interface hardware and Acqknowledge software (version 3.8.1).

Table 1. Composition and properties of modified Cortland salines (Wolf, 1963) used in the Ussing chamber experiments

	Serosal (mmol l^{-1})	Mucosal (mmol l^{-1})
NaCl	124.1	124.1
KCl	5.0	5.0
$CaCl_2$	1.6	1.6
$MgSO_4$	0.9	0.9
NaH_2PO_4	3.0	–
Na_2HPO_4	–	3.0
$NaHCO_3$	6.5	–
Glucose	0.1%	–
Mannitol	–	10
Gas	0.3% CO_2 in O_2	O_2
pH	7.8	7.8
Osmolality	280	280

The mucosal saline was titrated to pH 7.8 with NaOH.

Electrophysiological measurements were performed under symmetric conditions (see Grosell and Genz, 2006) using voltage clamp (0 mV) with mucosal reference while current was recorded. A 5 mV potential was induced for 3 s, at 60 s intervals, through the epithelium from the mucosal to the serosal side. Current and voltage data obtained together with the area of the exposed tissue permitted the calculation of epithelial conductance as follows:

$$G = I / (V \times A) , \quad (1)$$

where G is conductance (μS cm^{-2}), I is current, V is electrical potential and A is tissue area. The saline in the mucosal chamber was then removed and the chamber rinsed and refilled with mucosal saline (1.6 ml), and gassed with O_2 for stable titrations. During the course of the flux experiments described below, G and transepithelial potential (TEP) were measured under current-clamp conditions with 50 μA pulses (3 s) every 60 s.

For base and ammonia flux measurements, the preparations were maintained under asymmetric, current-clamp conditions in the absence of pH and osmotic gradients. The pH electrode and microburette of the pH-stat system were inserted into the mucosal chamber to measure the net base flux using a pH-stat technique (Grosell and Genz, 2006). In brief, the mucosal salines were maintained at 7.800±0.003 pH units by the addition of 0.005 mol l^{-1} HCl, as measured with combination pH electrodes (PHC4000.8, Radiometer, Copenhagen, Denmark) and titrated with auto-microburettes, both connected to pH-stat titration systems (TIM 854 or 856, Radiometer). The titration data were transferred to a PC using Titramaster software (versions 1.3 and 2.1) for further analysis, and base secretion rate (J_{base}) was calculated as:

$$J_{base} = H^+ / (A \times t) , \quad (2)$$

where H^+ is the amount of 0.005 mol l^{-1} HCl added by the pH-stat system over time (t) in 1 h intervals per area (A) of tissue insert (cm^2). Net base flux is expressed as μequiv cm^{-2} h^{-1}. Positive values indicate a net base flux into the mucosal compartment.

An initial 1 h control flux with stable TEP and base secretion rates was followed by a 2 h experimental flux period with 10 mmol l^{-1} NH_4Cl on the serosal side added as a 100× stock solution, and finally

by a 2 h experimental flux with 10 mmol l^{-1} NH_4Cl on the serosal side and a pharmacological inhibitor on either the mucosal or the serosal side (see below). Osmotic gradients were eliminated by compensation with mannitol. The ammonia gradient, 10 mmol l^{-1} NH_4Cl, used throughout the assays is within the range experienced by this animal as plasma and tissue values higher than 15 mmol l^{-1} have been measured (Chew et al., 2001; Moreira-Silva et al., 2010; Tsui et al., 2002).

A set of fluxes (N=3) was also made without the pH-stat set-up and base was allowed to accumulate in the mucosal saline over a 2 h period. Total HCO_3^- and CO_3^{2-} were then measured as titratable alkalinity by double end-point titration as described previously (Grosell and Genz, 2006).

In addition, ammonia flux rates were measured following reversal of the ammonia gradient. After the initial 1 h control flux, the 2 h experimental flux with 10 mmol l^{-1} NH_4Cl on the serosal side was followed by a final 2 h with no ammonia on the serosal side and 10 mmol l^{-1} NH_4Cl on the mucosal side. Net base fluxes were not measured in this series of experiments because the serosal saline was gassed with 0.3% CO_2/O_2, which would have interfered with the pH-stat titration.

The inhibitors used were as follows (all from Sigma-Aldrich, St Louis, MO, USA): ouabain [1β,3β,5β,11α,14,19-hexahydroxycard-20(22)-enolide 3-(6-deoxy-α-L-mannopyranoside)]; DIDS (4,4′-diisothiocyano-2,2′-stilbene-disulfonic acid); EIPA [5-(*N*-ethyl-*N*-isopropyl) amiloride]; and ethoxzolamide (ETZ). Ouabain is a specific inhibitor of Na^+/K^+-ATPase (Silva et al., 1977), and was added to the serosal saline at a final concentration of 1 mmol l^{-1} as a 100× stock solution. DIDS is a non-specific HCO_3^- transport inhibitor that has been demonstrated to reduce Cl^- influx and cause alkalosis by inhibiting Cl^-/HCO_3^- exchange (Cabantchik et al., 1972), and was used in the mucosal saline at a final concentration of 0.1 and 1.0 mmol l^{-1} as an 8× stock solution, carefully adjusted to pH 7.8. EIPA is a potent inhibitor of NHE (Kleyman et al., 1988). In the present study, EIPA was added to the mucosal saline at a final concentration of 0.1 mmol l^{-1} from a 100× stock in vehicle [45% (w/v) 2-hydroxypropyl-β-cyclodextrin (0.5% final concentration)]. ETZ is a permeant CA inhibitor and was used in the serosal saline at a concentration of 0.1 mmol l^{-1} [200× (20 mmol l^{-1}) stock solution in ethanol; 0.5% final concentration] (Maren, 1977). All the inhibitor stocks used in this study were also recently used in similar *in vitro* studies on toadfish and trout, which confirmed their efficacy (Grosell and Genz, 2006; Grosell et al., 2009a; Genz et al., 2011).

During the course of the experiments, mucosal saline samples (200 µl) were taken every 30 min for ammonia measurements and replaced with fresh mucosal saline. The serosal saline was changed at 2 h intervals, the only exception being during the reversal experiment, when serosal saline samples were taken for the measurement of ammonia flux in the reverse direction. Total ammonia was measured as detailed elsewhere (Verdouw et al., 1978) and ammonia flux rates were calculated taking into consideration the effects of sampling on saline volume in the half chambers. The potential interference of pharmacological agents and vehicle in the assay was determined and corrective measures taken when appropriate. In initial tests, the commonly used vehicle DMSO was found to interfere with the ammonia assay and was, therefore, not used. Ammonia flux rates (J_{amm}) were calculated as:

$$J_{amm} = \Delta TAN / (A \times t) , \quad (3)$$

where ΔTAN represents the accumulation of total ammonia nitrogen in the mucosal saline (with the exception of the reverse gradient experiment, in which ammonia was measured in the serosal saline) corrected for time (t) in hours and the two-dimensional area (A) of the tissue insert (cm^2). Ammonia flux rates are expressed as µmol cm^{-2} h^{-1} and positive values indicate net ammonia excretion into the mucosal saline.

Saline [NH_3], [NH_4^+] and NH_3 partial pressure (P_{NH_3}) were calculated from [TAN] and pH measurements using the Henderson–Hasselbalch equation with dissociation constant (pK_a) and ammonia solubility coefficient (αNH_3) values for trout plasma at 25°C from Cameron and Heisler (Cameron and Heisler, 1983). The P_{NH_3} gradient across the intestinal preparations (ΔP_{NH_3}) was calculated as:

$$\Delta P_{NH_3} = P_{ser,NH_3} - P_{muc,NH_3} , \quad (4)$$

where P_{ser,NH_3} is the P_{NH_3} in the serosal saline and P_{muc,NH_3} is the P_{NH_3} in the mucosal saline. Positive values favor serosal to mucosal ammonia flux rates.

The Nernst potential for NH_4^+($E_{NH_4^+}$) was calculated as:

$$E_{NH_4^+} = RTzF \ln ([NH_4^+]_{muc} / [NH_4^+]_{ser}) , \quad (5)$$

where R is the gas constant, T is the absolute temperature, z is the valency, F is Faraday's constant, and $[NH_4^+]_{ser}$ and $[NH_4^+]_{muc}$ are the concentrations of NH_4^+ in the serosal saline and mucosal saline, respectively. The true electrochemical potential or net driving force ($F_{NH_4^+}$) for NH_4^+ across the intestinal epithelium was calculated as:

$$F_{NH_4^+} = E_{NH_4^+} - TEP . \quad (6)$$

Positive $F_{NH_4^+}$ values favor serosal to mucosal ammonia flux and negative $F_{NH_4^+}$ values favor mucosal to serosal ammonia flux.

Histological analysis

To assess tissue integrity at the end of each experiment, insert mounted tissues were fixed *in situ* in 3% paraformaldehyde/phosphate-buffered saline (pH 7.3) overnight at 4°C. Tissue was processed for paraffin embedding, cross-sectioned (5 µm), and stained with the periodic acid–Schiff (PAS) method, Alcian Blue (pH 2.5) and 1% Gill's hematoxylin (Merck, Whitehouse Station, NJ, USA). Sections were viewed and photographed with a Leica DM6000B photomicroscope.

Ammonia and air exposure experiment

Fish (5.70±1.89 g and 9.4±1.6 cm, means ± s.d.) for tissue collection were divided into three groups (22 animals in each group) and acclimated under control conditions (dechlorinated tap water), high ammonia (30 mmol l^{-1} NH_4Cl at pH 7.2 and 21°C in dechlorinated tap water, corresponding to 200 µmol l^{-1} NH_3) or aerial exposure (1 ml of dechlorinated tap water) for 7 days, similar to conditions described previously (Tsui et al., 2002). At the end of the experiment the fish were overdosed with neutralized tricane methanesulfonate [1:5000 (w/v)] and killed by decapitation; anterior and posterior intestinal tissues were excised and immediately frozen in liquid nitrogen, and stored at −80°C for posterior intestine membrane fluidity measurements.

Gut membrane fluidity

Plasma membranes from intestine were purified by density gradient centrifugation (Daveloose et al., 1993). In brief, samples were pooled into three groups (each group pooled from 7–8 samples) and homogenized in isolation medium (300 mmol l^{-1} sucrose, 10 mmol l^{-1} Tris-HCl, 1 mmol l^{-1} DTT), 1:4 (w:v), with a glass Dounce homogenizer (pestle A) on ice. The membranes were separated on a sucrose step gradient at 100,000 relative centrifugal force (RCF; Beckman Coulter Optima Max with an MLS-50 swinging-bucket

rotor; Beckman Coulter, Fullerton, CA, USA). To determine membrane enrichment and purity, total protein was determined by the bicinchoninic acid method (Smith et al., 1985) and Na^+/K^+-ATPase and lactate dehydrogenase activities measured according to established protocols (Katynski et al., 2004). Membrane fluidity was measured using a fluorimetric method (fluorescence anisotropy) (Katynski et al., 2004). In brief, fluorescence anisotropy of the probe 1,6-diphenyl-1,3,5-hexatrienyl-propionic acid (DPH) incubated with the membranes was measured with a POLARstar Galaxy microplate fluorometer (BMG Labtech, Frankfurt, Germany), with excitation and emission monochromators set at 360 and 430 nm, respectively, in a temperature gradient (27, 29, 34, 37 and 39°C). The anisotropy of the probe DPH gives an indication of lipid order, with higher anisotropy corresponding to a more ordered membrane. A more ordered membrane is predicted to be less permeable (Kikeri et al., 1989; Lande et al., 1995; Katynski et al., 2004).

Statistical analysis

Results are presented as means ± s.e.m. Two-way repeated measures ANOVA followed by Student–Newman–Keuls *post hoc* test was used for electrophysiology, pH-stat and ammonia flux analysis because two independent factors (tissue and treatment) affected the tested response. For two group comparisons, *t*-tests were performed (SigmaStat 3.0, SPSS, Chicago, IL, USA). Membrane fluidity linear regressions were compared by ANCOVA (R software). Values were considered significantly different at $P<0.05$.

RESULTS

Electrophysiological properties of anterior and posterior intestine

The conductance (G) and short circuit current (I_{sc}) were significantly higher in the anterior intestine than in the posterior intestine (2.5- and 9.4-fold, respectively). No differences were found between intestinal regions with regards to the TEP (Table 2). Both conductance and TEP were stable over the experimental time course under current-clamp conditions in preliminary experiments (supplementary material Fig. S1). Only after 5 h did TEP in the posterior intestine and conductance in the anterior intestine increase significantly relative to the pre-TAN control period. In agreement, histological examination of the mounted tissue indicated that tissue integrity was maintained (Fig. 1).

Net ammonia and base flux

In all experiments, net ammonia flux rates under control conditions were higher in anterior (0.32±0.07 μmol cm^{-2} h^{-1}) than in posterior intestine (0.06±0.00 μmol cm^{-2} h^{-1}), and in some cases flux rates in the posterior intestine were below the detection limit. In order to have a consistent ammonia efflux, 10 mmol l^{-1} TAN was added to the serosal side, and the net ammonia flux increased significantly to 1.07±0.30 μmol cm^{-2} h^{-1} in the anterior intestine, and to 0.96±0.26 μmol cm^{-2} h^{-1} in the posterior intestine. In the anterior and posterior intestine, respectively, the calculated serosal–mucosal gradients for NH_4^+ (ΔNH_4^+) were 9.41±0.07 and 9.64±0.06 mmol l^{-1}, and for NH_3 (ΔNH_3) they were 0.303±0.002 and 0.311±0.001 mmol l^{-1}. The measured TEPs were −0.83±0.63 and −0.55±0.68 mV, respectively, and calculated equilibrium potentials for NH_4^+ (E_{NH4}^+) were −97.66±2.74 and −123.47±4.97 mV, respectively. The calculated NH_4^+ driving forces (F_{NH4}^+) were −98.21±2.58 and −122.29±5.65 mV for anterior and posterior intestine, respectively. These calculations indicate strong serosal to mucosal gradients in both preparations. In preliminary experiments, the net ammonia flux remained stable over a 4 h period (maximum length of experimental protocols) at high serosal TAN.

Because of the relatively small sample number in individual experiments, all the flux data from control and 10 mmol l^{-1} serosal ammonia periods are summarized in Table 3. During the initial control flux, net base flux rates were significantly greater in the anterior than in the posterior intestine. Application of the 10 mmol l^{-1} TAN serosal–mucosal gradient resulted in a significant decrease in net base flux rate in the anterior intestine after 2 h, while a significant increase was observed in the posterior intestine at both 1 and 2 h. There were no differences in base flux between the anterior and posterior intestine with the 10 mmol l^{-1} serosal–mucosal ammonia gradient. In preliminary experiments, net base flux remained stable over a 6 h period.

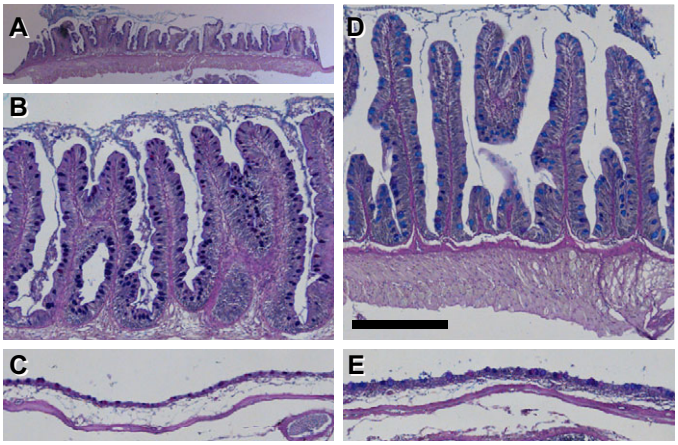

Fig. 1. Histological sections of anterior (A,B,D) and posterior (C,E) intestinal preparations mounted in the Ussing chambers. Micrographs A–C are from a control preparation and micrographs D–E are from preparations exposed to 1.0 mmol l^{-1}ouabain. Sections are stained with Alcian Blue (pH 2.5), periodic acid–Schiff and Gils hematoxylin. Scale bars, 1.5 mm (A), 250 μm (B–E).

Table 2. Electrophysiological properties of the weatherloach anterior and posterior intestine under symmetrical conditions during current clamp and voltage clamp

Intestinal region	G (μSi cm^{-2})	I_{sc} (μA cm^{-2})	TEP (mV)
Anterior	9.24±0.19	22.61±2.41	2.64±0.29
Posterior	3.65±0.46	7.41±1.75	2.50±0.83
P-value	0.008	<0.001	0.869

Values are means ± s.e.m. (N=4) (*t*-test *P*-values are shown).
G, conductance; I_{sc}, short-circuit current; TEP, transepithelial potential.

Table 3. Summary of base flux rates (μequiv cm^{-2} h^{-1}) under control and serosal 10 mmol l^{-1} TAN (1 and 2 h) conditions pooled from inhibitor experiments

		TAN	
Intestine region	Control	1 h	2 h
Anterior	0.802±0.068^{a}	0.654±0.049^{a,b}	0.507±0.058^{b}
Posterior	0.303±0.125^{A,*}	0.567±0.163^{B}	0.595±0.122^{B}

Data were analyzed by two-way repeated measures ANOVA (N=11). Within a given tissue, groups with different uppercase/lowercase letters are significantly different.
*Significant difference from anterior intestine.
TAN, total ammonia nitrogen.

The HCO_3^- flux rates measured by double end-point titration of the accumulated HCO_3^- equivalents over a 2 h period in the absence of pH-stat titration were 0.569±0.101 and 0.062±0.129 μmol cm^{-2} h^{-1} for anterior and posterior intestine, respectively. Rates were significantly higher in the anterior intestine (P=0.045; paired t-test). In the anterior intestine over 70% of overall base flux could be accounted for by HCO_3^- equivalents; however, in the posterior intestine less than 10% was accounted for in this way. After 2 h, the mucosal pH increased to 8.027±0.031 and 7.780±0.091 in the anterior and posterior intestine, respectively (P=0.061) from an initial pH 7.742±0.021.

Pharmacological effects

In the anterior intestine, the addition of the Na^+/K^+-ATPase inhibitor ouabain to the serosal saline, in the presence of the 10 mmol l^{-1} serosal–mucosal TAN gradient, caused a significant decrease in the net ammonia flux of 54% (Fig. 2A). No significant difference was observed in the posterior intestine. There were also significant decreases in the net base flux in the anterior intestine (37–46%) with no significant changes in the posterior intestine (Fig. 2B). During this experiment TEP gradually decreased in both intestinal regions (supplementary material Fig. S2). Ouabain had no effect on anterior intestine conductance; however, in the posterior intestine, conductance increased significantly in the final hour of treatment.

The chloride transport inhibitor DIDS added to the mucosal saline at a dose of 0.1 mmol l^{-1} had no effect on net ammonia flux in either the anterior or the posterior intestine (Fig. 3A). However, the higher dose of 1.0 mmol l^{-1} DIDS inhibited the ammonia flux by 53% and 87%, respectively. There was a significant decrease in the net base flux in the anterior intestine of up to 66% during the course of DIDS exposure, while no effect was observed in the posterior intestine (Fig. 3B). DIDS had no effect on either TEP or conductance in either intestinal region (supplementary material Fig. S3).

The NHE-specific inhibitor EIPA significantly decreased the ammonia flux rate in both the anterior and the posterior intestine by 74% and 71%, respectively, when added to the mucosal side (Fig. 4A). No effect of EIPA on base excretion was detected in either intestinal region (Fig. 4B). EIPA had no effect on conductance in the anterior intestine but in the posterior intestine, conductance increased gradually during the treatment. In the posterior intestine, TEP was variable during the course of the experiment but the only significant difference was between the 1 h EIPA treatment and 1 h TAN groups. No significant changes in anterior intestine TEP were observed (supplementary material Fig. S4).

The CA inhibitor ETZ had no effect on net base flux (Fig. 5) in either the anterior or the posterior intestine. J_{amm} data are not presented, as loss of some samples prevented statistical analysis. ETZ had no effect on anterior intestine conductance or TEP; however, in the posterior intestine, conductance increased markedly (supplementary material Fig. S5). No changes in posterior intestine TEP were observed.

Reversal of the ammonia gradient

Following the removal of the 10 mmol l^{-1} TAN from the serosal side and the addition of ammonia with the same concentration to the mucosal side, the NH_3 and NH_4^+ gradients and $F_{NH_4^+}$ were reversed (Table 4). However, the absolute magnitude of the reversed ΔNH_3 was lower because pH differences developed in the absence of the pH-stat system but were still comparable between intestinal regions. When comparing the absolute magnitude of the net ammonia flux rates, thus irrespective of direction (serosal–mucosal *versus* mucosal–serosal), there was no difference in the anterior intestine. However, in the posterior intestine a significant decrease (49%) was observed (Fig. 6) even though NH_3 and NH_4^+ gradients and $F_{NH_4^+}$ would predict otherwise. Ammonia gradient reversal resulted in opposite effects on epithelial conductance with a significant decrease in the anterior intestine and a significant increase in the posterior intestine (supplementary material Fig. S6). Posterior intestine TEP also increased significantly while no significant difference was observed in the anterior intestine.

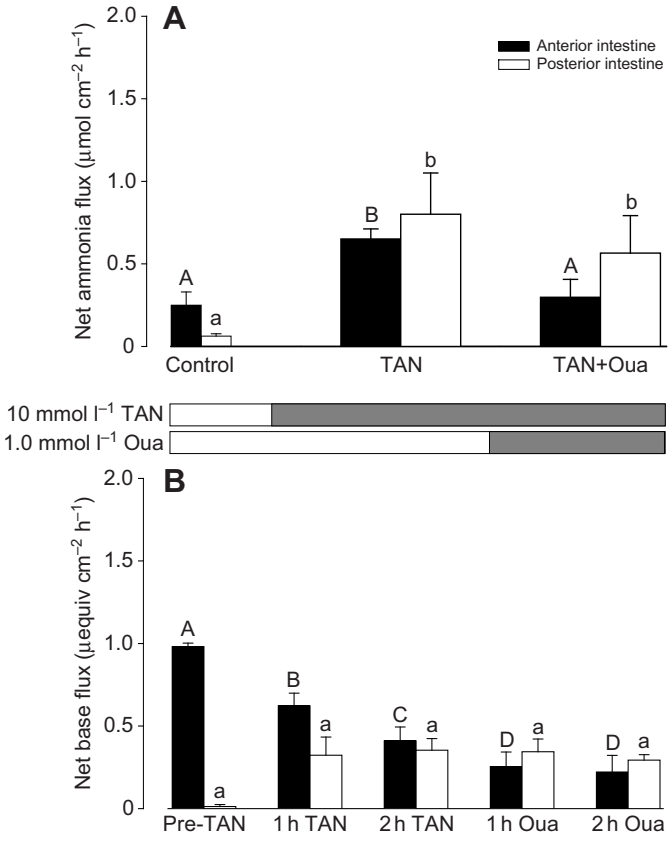

Fig. 2. Effect of serosal additional of the Na^+/K^+-ATPase inhibitor ouabain (Oua, 1 mmol l^{-1}) on (A) net ammonia flux rates and (B) net base flux rates in the presence of a 10 mmol l^{-1} total ammonia nitrogen (TAN) serosal–mucosal gradient in *Misgurnus anguillicaudatus* anterior and posterior intestine. Values are means + s.e.m. (N=4). Bars with different uppercase/lowercase letters are significantly different (P<0.05).

Gut membrane fluidity

Anisotropy was temperature dependent and regressions of control, ammonia and aerial exposure were parallel. Posterior intestine fluorescence anisotropy was found to be higher, thus indicating lower membrane fluidity, in the HEA (intercept=0.234+0.024, P<0.02) and air-exposed fish (intercept=0.234+0.022, P<0.04) compared with control (intercept=0.234). The insufficient number of pooled anterior intestine samples did not allow us to determine statistical differences between the exposure groups. However, a trend similar to that of the posterior intestine, with the regression lines of HEA and air-exposed groups positioned above the control regression line, indicates lower membrane fluidity than controls as well.

DISCUSSION

Ammonia transport involving the Na^+/K^+-ATPase and NHE is demonstrated by the pharmacological inhibition of the net ammonia

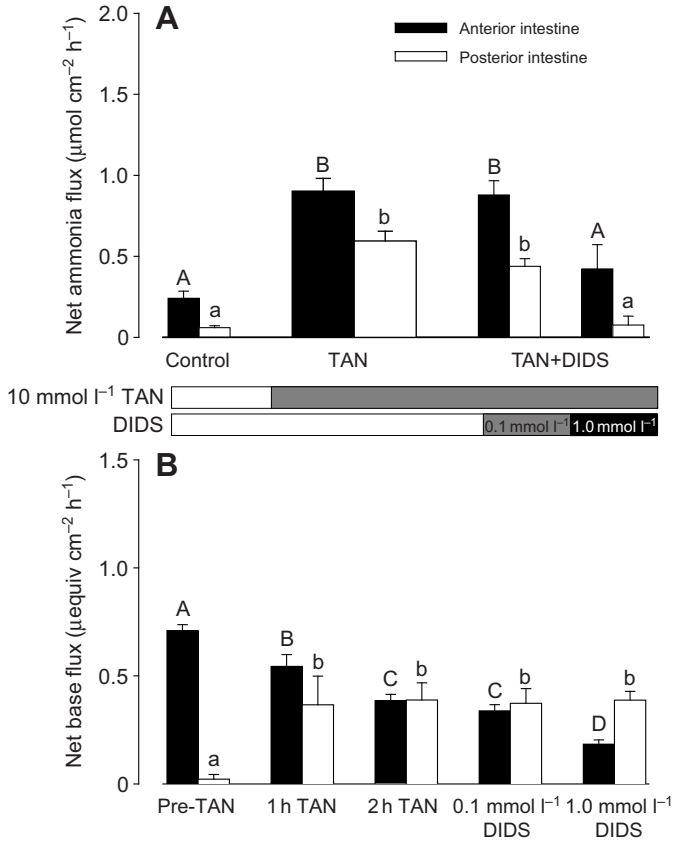

Fig. 3. Effect of mucosal addition of the chloride transport inhibitor DIDS (0.1 and 1.0 mmol l^{-1}) on (A) net ammonia flux rate and (B) net base flux rate in the presence of a 10 mmol l^{-1} TAN serosal–mucosal gradient in *M. anguillicaudatus* anterior and posterior intestine. Values are means + s.e.m. (*N*=4). Bars with different uppercase/lowercase letters are significantly different (*P*<0.05).

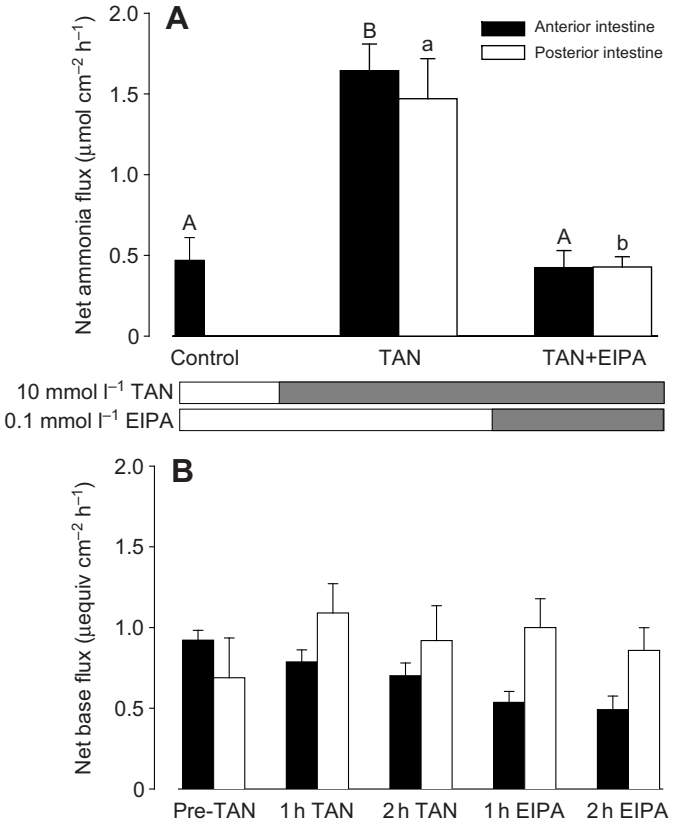

Fig. 4. Effect of mucosal addition of the Na^+/H^+ exchanger inhibitor EIPA (0.1 mmol l^{-1}) on (A) net ammonia flux rate and (B) net base flux rate in the presence of a 10 mmol l^{-1} TAN serosal–mucosal gradient in *M. anguillicaudatus* anterior and posterior intestine. Values are means + s.e.m. (*N*=4). Bars with different uppercase/lowercase letters are significantly different (*P*<0.05).

excretion rate with ouabain and EIPA, respectively in the loach gut. The intestinal lumen alkalinization can be attributed to a DIDS (a non-specific HCO_3^- transport inhibitor)-sensitive net base (HCO_3^-) flux in the anterior intestine, an important component of the proposed ammonia volatilization mechanism. Base flux under a serosal–mucosal ammonia gradient was not dependent on CA, as indicated by a lack of inhibition with ETZ. Membrane fluidity of the posterior intestine was lower in HEA and air-exposed fish than in controls, which correlates with lower ammonia membrane permeability, as was evident from the lower ammonia flux rate in the reversed ammonia gradient experiment (see Fig. 7).

In the present study, TEP in the anterior and posterior intestine under symmetrical conditions was not different; however, conductance (G) and I_{sc} were higher in the former. These differences are in line with the striking morphological and functional differences in these regions, with the anterior intestine being a more active zone of the gut with a clear digestive and absorptive role and the posterior intestine having a clear function in respiratory gas exchange (McMahon and Burggren, 1987; Gonçalves et al., 2007). These differences are also in agreement with the proposed transporter-facilitated NH_4^+ excretion in the anterior intestine.

The NHE is implicated in gut ammonia excretion as EIPA (NHE inhibitor) decreased ammonia flux rate in both the anterior and the posterior intestine. Although it was not possible to measure intestinal lumen Na^+ levels in the loach, values measured in low salinity (2.5 p.p.t.)-acclimated toadfish *Opsanus beta* (McDonald and Grosell, 2006) and post-prandial freshwater tilapia (Grosell, 2007) and rainbow trout (Bucking and Wood, 2006; Bucking and Wood, 2009) were within the range of the mucosal saline Na^+ concentrations used in this study. Thus, a favorable apical Na^+ electrochemical gradient would be present to drive the exchange. While our study is the first to demonstrate a role for fish intestinal NHE in ammonia excretion, there is ample evidence suggesting a direct or indirect role of NHE in gill ammonia excretion in aquatic organisms. *In vivo* exposure of *Periophthalmodon schlosseri* to 10^{-4} mol l^{-1} amiloride (a non-specific NHE inhibitor) induced a decrease in net ammonia excretion, indicating NHE involvement in ammonia excretion (Randall et al., 1999). In *Oncorhynchus mykiss* exposed to 0.5 mmol l^{-1} and 1.0 mmol l^{-1} amiloride, a decrease in ammonia excretion by 58% and 87%, respectively, was observed but not with a lower dose of 0.1 mmol l^{-1} amiloride (Lin and Randall, 1991). In a study by Wilson and co-workers, *O. mykiss* exposure to amiloride (10^{-4} mmol l^{-1}) did not indicate the presence of direct Na^+/NH_4^+ exchange; nevertheless, it decreased net ammonia flux by ~20% (Wilson et al., 1994). These studies were all performed *in vivo* and the inhibitors were added to the water, which implies that they were affecting gill apical NHE. However, similar *in vivo* inhibitor studies in loach with 10^{-4} mol l^{-1} amiloride had no effect on ammonia excretion rates (Moreira-Silva et al., 2010). Instead, as demonstrated in a number of other fishes, indirect coupling of an apical H^+-ATPase and Rhesus (Rh)

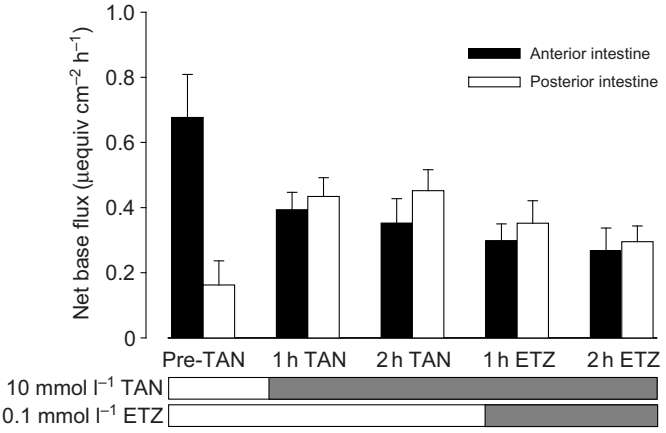

Fig. 5. Effect of serosal addition of the carbonic anhydrase inhibitor ETZ (0.1 mmol l^{-1}) on net base flux rate in the presence of a 10 mmol l^{-1} TAN serosal–mucosal gradient in *M. anguillicaudatus* anterior and posterior intestine. Values are means + s.e.m. (*N*=6). Bars with different uppercase/lowercase letters are significantly different (*P*<0.05).

glycoprotein ammonia transporters facilitate branchial ammonia excretion (Weihrauch et al., 2009; Wright and Wood, 2009). However, recent studies in the yolk sac skin (surrogate gill ionocyte model) of larval fish give the best detailed mechanistic evidence of the role of the NHE in ammonia excretion (Shih et al., 2008; Shih et al., 2012; Wu et al., 2010; Kumai and Perry, 2011). In zebrafish larvae skin, although the H^+-ATPase still dominates the proton flux (80%) (Shih et al., 2008), *NHE3b* gene knockdown and EIPA have also been shown to decrease the proton gradient that drives facilitated NH_3 diffusion by an acid-trapping mechanism through the apical Rh glycoprotein ammonia transporter Rhcg1 under low sodium (Shih et al., 2012) and low pH (Kumai and Perry, 2011) conditions when *NHE3b* expression is enhanced. Significantly, ammonia excretion has been found to drive Na^+ uptake *via* NHE under these conditions (Shih et al., 2012; Kumai and Perry, 2011). In contrast to zebrafish, in larval medaka skin, NHE is the dominate proton excretory mechanism linked to Rhcg1-mediated ammonia excretion (Wu et al., 2010). Evidence of direct Na^+ and NH_4^+ exchange *via* NHE in fish gill is lacking although in mammalian kidney proximal tubule, NHE3 functions directly in Na^+ and NH_4^+ exchange in the absence of RhCG expression (Weiner and Verlander, 2011). In the loach intestine, it remains to be determined whether the EIPA-sensitive NHE is acting directly in Na^+/NH_4^+ exchange or functions as a Na^+/H^+ exchanger coupled to an apical Rh ammonia transporter.

In the anterior intestine, ouabain inhibition of Na^+/K^+-ATPase decreased net ammonia flux by 54%, demonstrating that the ion transporter Na^+/K^+-ATPase is involved in ammonia excretion. This may be a direct role through the basolateral uptake of NH_4^+ in place of K^+ in exchange for Na^+ by the ATPase, which has been demonstrated in the gills of the giant mudskipper, *P. schlosseri* (Randall et al., 1999), the oyster toadfish, *O. beta* (Mallery, 1983) and the blue crab, *Callinectes ornatus* (Garçon et al., 2007). However, Na^+/K^+-ATPase may play an additional or alternative indirect role through the maintenance of cell electronegativity and low intracellular Na^+. In this way, the inward Na^+ electrochemical gradient would drive apical NH_4^+ excretion *via* NHEs. An increase in intestinal epithelial resistance with ouabain treatment in goldfish intestine has been demonstrated and linked to the collapse of the lateral intercellular spaces (Albus et al., 1979), which might suggest a similar effect in loach, whereby the paracellular pathway is blocked thereby decreasing ammonia flux. However, in loach neither changes in anterior intestine conductance nor changes in epithelial morphology (collapse of lateral intercellular spaces) were observed with ouabain treatment. Also, the increase in conductance (decrease in resistance) of the posterior intestine with ouabain did not correlate with changes in J_{amm}. The preferential effects of ouabain in the anterior intestine are reflected by the observation that tissue expression levels of Na^+/K^+-ATPase α-subunit, determined by immunoblotting and immunohistochemistry, are much higher in this gut region than in the posterior intestine (Gonçalves et al., 2007) (J.C.M.-S. and J.M.W., unpublished observation).

The base flux in the loach anterior and posterior intestine in the absence of imposed ammonia gradients was 0.802 and 0.303 μequiv cm^{-2} h^{-1}. Although on the high side, these rates are comparable to those measured in marine [0.5 μequiv cm^{-2} h^{-1} (see Grosell, 2010)] and freshwater [0.3 μequiv cm^{-2} h^{-1} (Genz et al., 2011)] fishes. The high anterior intestinal flux rates may reflect the fact that the gut of the loach is straight and very short, and as the anterior region represents only one-fifth of this length, the transport capacity must be accommodated into a relatively small area. The findings were also surprising given that the loach is agastric and, therefore, does not need intestinal base secretion to neutralize gastric acid secretion as in the marine species studied (Taylor et al., 2011; Wilson et al., 2011).

DIDS was effective in inhibiting HCO_3^- excretion at 10^{-3} mol l^{-1} as has been demonstrated in *Platichthys flesus* (Grosell and Jensen, 1999) and *O. mykiss* (Grosell et al., 2009a), although in *Anguilla japonica* (Ando and Subramanyam, 1990) and *Citharichthys sordidus* (Grosell et al., 2001) the lower dose of 10^{-4} mol l^{-1} was effective, but not in *Gillichthys mirabilis* (Dixon et al., 1986). At

Table 4. Calculation of transepithelial gradients

	ΔNH_4^+ *,** (mmol l^{-1})	ΔNH_3 * (mmol l^{-1})	$E_{NH_4^+}$ ** (mV)	TEP *,** (mV)	$F_{NH_4^+}$ **
Anterior$_{s-m}$	9.10±0.04	0.30±0.00	–95.57+4.19	0.16±0.43	–95.72+3.83
Posterior$_{s-m}$	9.27±0.05	0.31±0.00	–137.18+13.71	1.22±0.60	–138.4+13.93
Anterior$_{m-s}$	–9.47+0.12	–0.16+0.02	136.96±17.76	0.94±0.46	136.02±17.50
Posterior$_{m-s}$	–9.68+0.04	–0.13+0.04	173.11±11.12	3.06±0.63	170.05±10.86

Transepithelial gradients of NH_4^+(ΔNH_4^+) and NH_3 (ΔNH_3), and the Nerst equilibrium potential ($E_{NH_4^+}$), transepithelial potential (TEP) and driving force ($F_{NH_4^+}$) across the anterior and posterior intestine preparations with nominal 10 mmol l^{-1} TAN serosal to mucosal (s–m) and reversed 10 mmol l^{-1} TAN mucosal to serosal (m–s) gradients. A positive value for ΔNH_4^+ or ΔNH_3 would favor ammonia flux in the serosal–mucosal direction, while a negative value would favor mucosal–serosal movement. Negative $F_{NH_4^+}$ values would favor serosal–mucosal NH_4^+ flux. Gradients were averaged over the flux periods (*N*=4). Absolute data values were analyzed by 2-way ANOVA.

*Significant difference between serosal–mucosal and mucosal–serosal gradients; **significant difference between anterior and posterior intestine.

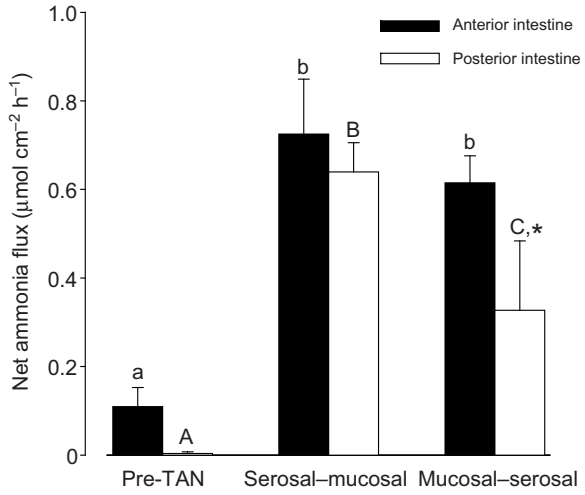

Fig. 6. Effect of ammonia gradient reversal from a 10 mmol l^{-1} TAN serosal–mucosal to a 10 mmol l^{-1} TAN mucosal–serosal gradient on corresponding serosal–mucosal and mucosal–serosal ammonia net flux rates in *M. anguillicaudatus* anterior and posterior intestine. Note that flux rates are presented as absolute values, and are thus irrespective of direction. Data are presented as means + s.e.m. (N=3). Bars with different uppercase/lowercase letters are significantly different (P<0.05). *Significant difference from anterior intestine.

the lower dose of 10^{-5} mol l^{-1} DIDS, inhibition of HCO_3^- excretion was also not observed in *O. mykiss* (Wilson et al., 1996). It has been noted that the preparation of DIDS is key to its efficacy (Grosell et al., 2009b), and such precautions were taken in the present study. We thus conclude that the HCO_3^- excretion mechanism is relatively DIDS insensitive in loach and similar to that seen in trout and flounder (Grosell et al., 1999; Grosell et al., 2009a).

The DIDS inhibition of the *in vitro* ammonia flux may in part be explained by the indirect acid–base effects on epithelial cells and the apical boundary layer. There is evidence that DIDS can inhibit ammonia flux indirectly through inhibition of the sodium–bicarbonate co-transporter (NBC) in kidney medullary thick ascending limb and lung alveolar cells (Tokuda et al., 2007; Lee et al., 2010). In erythrocytes, Garcia-Romeu and colleagues demonstrated a DIDS-sensitive K^+ flux (Garcia-Romeu et al., 1991) and, given the promiscuity of K^+ transporters for NH_4^+ (Knepper et al., 1989), DIDS may be acting directly on ammonia flux. Although DIDS has been shown to inhibit Na^+/K^+-ATPase activity *in vitro* (Faelli et al., 1984), this would be unlikely in the present study because of the inaccessibility of cytosolic binding sites for DIDS, which is membrane impermeable.

In the weatherloach volatilization model, we predicted the involvement of a cytosolic and an extracellular CA in the respective intracellular hydration of CO_2 to form HCO_3^- and the luminal dehydration of HCO_3^- into CO_2. However, the lack of effect of ETZ, a permeant inhibitor that would inhibit both intracellular and extracellular luminal CA, argues against a role for these proteins in net base and ammonia flux in the weatherloach, and that uncatalyzed rates of reaction are sufficient under high ammonia conditions. In contrast, in the marine toadfish (Grosell and Genz, 2006) and seawater-acclimated rainbow trout (Grosell et al., 2009a), using ETZ Grosell and colleagues demonstrated that cytosolic CA and, thus, catalyzed endogenous HCO_3^- production are important to HCO_3^- secretion. Ando and Subramanyam reported similar findings in *A. japonica* using acetazolamide, another CA inhibitor (Ando and Subramanyam, 1990). However, in marine teleosts HCO_3^- secretion is a significant driver of Cl^- uptake and thus osmoregulation, which is not the case for teleosts living in fresh water (Grosell, 2010). As a corollary, in a study on the euryhaline rainbow trout, salinity acclimation resulted in an increase in cytosolic and membrane-bound CA isoforms (Grosell et al., 2007), which are involved in HCO_3^- secretion (Grosell et al., 2009a). Nevertheless, CA has been localized by enzyme histochemistry in the weatherloach digestive tract to both the 'stomach' (anterior intestine) and posterior intestine (Chang et al., 2006). Our results in the loach would indicate a role for transepithelial HCO_3^- secretion, making use of plasma HCO_3^- and a basolateral transporter such as NBC (Tokuda et al., 2007; Kurita et al., 2008), which is indirectly supported by the finding of ouabain-sensitive (Na^+/K^+-ATPase inhibited) net base flux in the anterior intestine. Similar effects of oubain on intestinal base secretion have been reported for the gulf toadfish intestine (Grosell and Genz, 2006). In addition, the uncatalyzed rates of CO_2 hydration may simply provide sufficient intracellular HCO_3^- that is not rate limiting

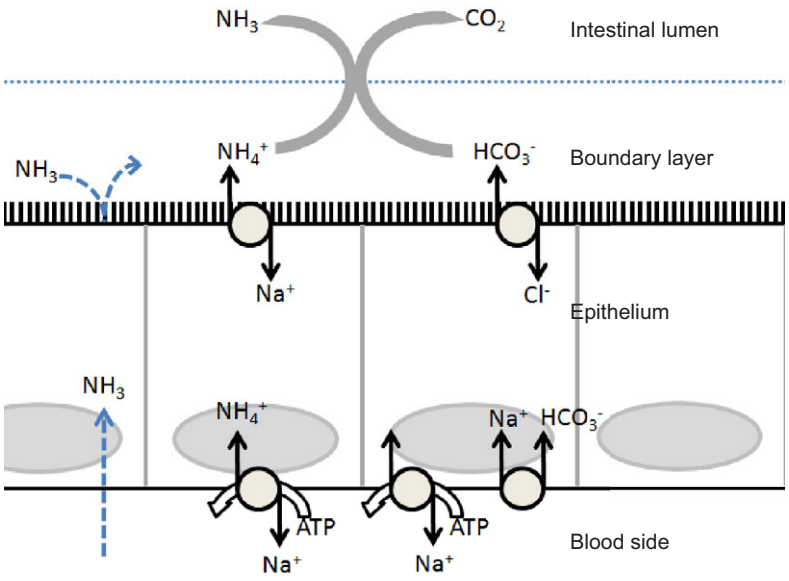

Fig. 7. Proposed model for gut alkalinization and ammonia volatilization through the gut of *M. anguillicaudatus*. The basolateral Na^+/K^+-ATPase, and apical Na^+/H^+ exchanger (NHE) and Cl^-/HCO_3^- anion exchanger are shown. A predicted basolateral Na^+:HCO_3^- co-transporter is also included. The molecular identity of these transporters and the potential involvement of Rhesus proteins await future work.

to base flux. The possibility that the high serosal ammonia levels resulted in an alkalinization of the epithelium (NH_3 diffusion) would also have decreased the importance of CA by directly driving CO_2 hydration ($NH_3 + CO_2 \rightarrow NH_4^+ + HCO_3^-$).

HEA (200 μmol l^{-1} NH_3) exposure and emersion both resulted in lower membrane fluidity in the posterior intestine. This increase in membrane order would decrease passive ammonia permeability, consistent with the results from the reversal of the 10 mmol l^{-1} TAN gradient from serosal–mucosal to mucosal–serosal, which significantly reduced the magnitude of the J_{amm}. These findings agree with the prediction that the intestinal epithelium has low permeability to NH_3 in order to minimize passive back flux. Low ammonia permeability of a number of epithelia, including gastric glands, kidney thick ascending limb and urinary bladder, has been correlated with high membrane order (Lande et al., 1995; Katynski et al., 2004; Kikeri et al., 1989; Singh et al., 1995). In other animals, environmental ammonia also induced changes in ammonia permeability at different sites such as the gill and skin. Ip and colleagues, using different approaches (including *in vitro* ammonia flux rates across a skin preparation in an Ussing chamber system, and cholesterol and fatty acid content analysis of skin), demonstrated that *P. schlosseri* skin has low permeability to NH_3 (Ip et al., 2004). The low skin permeability to NH_3 is reflected in the ability of this fish to maintain low plasma levels of ammonia against large inward gradients in conjunction with active excretion of ammonia through the gills *via* Na^+/K^+ (NH_4^+)-ATPase and NHE (Randall et al., 1999).

In summary, using an *in vitro* pharmacological approach, we have demonstrated that the mechanism of ammonia excretion in the anterior intestine of the loach involves an apical EIPA-sensitive NHE and basolateral Na^+/K^+-ATPase. The anterior intestine also has a significant net base secretion, which is largely HCO_3^-- and DIDS-sensitive, indicating a Cl^-/HCO_3^- exchange mechanism. These *in vitro* observations are consistent with the proposed mechanism of ammonia volatilization based on *in vivo* measurements (Tsui et al., 2002). NH_4^+ excreted by a NHE-dependent mechanism into the alkaline anterior intestinal boundary layer forms gaseous NH_3 and H^+. H^+ reacts excreted HCO_3^- forming gaseous CO_2 and both these gases can volatilize into the air, passing through the gut during intestinal breathing and thus avoiding a pH decrease associated with NH_3 formation. The HCO_3^- excretion also maintains the alkaline conditions (>pH 8) of the lumen surface layer, promoting NH_3 formation. The molecular identity of these transporters and the potential involvement of Rh proteins await future work.

LIST OF SYMBOLS AND ABBREVIATIONS

A	tissue area
CA	carbonic anhydrase
DIDS	4,4′-diisothiocyano-2,2′-stilbene-disulfonic acid
DPH	1,6-diphenyl-1,3,5-hexatrienyl-propionic acid
EIPA	5-(*N*-ethyl-*N*-isopropyl) amiloride
$E_{NH_4^+}$	Nernst potential for NH_4^+
ETZ	ethoxzolamide
F	Faraday's constant
$F_{NH_4^+}$	net driving force for NH_4^+
G	conductance
HEA	high environmental ammonia
I	current
I_{sc}	short-circuit current
J_{amm}	ammonia flux rate
J_{base}	base secretion rate
NBC	sodium–bicarbonate co-transporter
NH_3	un-ionized ammonia
NH_4^+	ammonium ion
NHE	Na^+/H^+ exchanger
pK_a	dissociation constant
P_{NH_3}	un-ionized ammonia partial pressure
R	gas constant
Rh	Rhesus
t	time
T	absolute temperature
TAN	total ammonia nitrogen
TEP	transepithelial potential
V	electrical potential
z	valency
αNH_3	un-ionized ammonia solubility coefficient

ACKNOWLEDGEMENTS

We would like Dr T. K. N. Tsui for procuring the fish and H. Santos and R. Gerdes for fish maintenance support. J.M.S. is currently working at 3B's Research Group – Biomaterials, Biodegradables and Biomimetics, University of Minho, Headquarters of the European Institute of Excellence on Tissue Engineering and Regenerative Medicine, Ave Park, 4806-909 Caldas das Taipas, Guimarães, Portugal, IBB – Institute for Biotechnology and Bioengineering, PT Government Associated Laboratory, Guimarães, Portugal.

FUNDING

This work was supported by a Fundação para a Ciência e a Tecnologia (FCT) grant [POCTI/BSE/47585/2002] to J.M.W. J.M.S. was supported by an FCT scholarship [SFRH/BD/16760/2004] and M.G. is supported by the National Science Foundation (NSF) [grant no. IOS 1146695]. This research was also partially supported by the European Regional Development Fund (ERDF) through the COMPETE–Operational Competitiveness Programme and national funds through the Foundation for Science and Technology (FCT) under the project PEst-C/MAR/LA0015/2011.

REFERENCES

Albus, H., Groot, J. A. and Siegenbeek van Heukelom, J. (1979). Effects of glucose and ouabain on transepithelial electrical resistance and cell volume in stripped and unstripped goldfish intestine. *Pflugers Arch.* **383**, 55-66

Ando, M. and Subramanyam, M. V. V. (1990). Bicarbonate transport systems in the intestine of the seawater eel. *J. Exp. Biol.* **150**, 381-394.

Bucking, C. and Wood, C. M. (2006). Gastrointestinal processing of Na^+, Cl^-, and K^+ during digestion: implications for homeostatic balance in freshwater rainbow trout. *Am. J. Physiol.* **291**, R1764-R1772.

Bucking, C. and Wood, C. M. (2009). The effect of postprandial changes in the pH along the gastrointestinal tract on the distribution of ions between the solid and fluid phases of chyme in rainbow trout. *Aquac. Nut.* **15**, 282–296.

Cabantchik, Z. I. and Rothstein, A. (1972). The nature of the membrane sites controlling anion permeability of human red blood cells as determined by studies with disulfonic stilbene derivatives. *J. Membr. Biol.* **10**, 311-330.

Cameron, J. N. and Heisler, N. (1983). Studies of ammonia in the trout: physicochemical parameters, acid–base behaviour and respiratory clearance. *J. Exp. Biol.* **105**, 107-125.

Chang, M.-H., Lo, D.-Y., Chou, C.-C. and Lee, W.-M. (2006). Distribution of carbonic anhydrase in digestive tract of pond loach (*Misgurnus anguilicaudatus*). *J. Vet. Med. Sci.* **68**, 1009-1011.

Chew, S. F., Jin, Y. and Ip, Y. K. (2001). The loach *Misgurnus anguillicaudatus* reduces amino acid catabolism and accumulates alanine and glutamine during aerial exposure. *Physiol. Biochem. Zool.* **74**, 226-237.

Daveloose, D., Vezin, H., Basse, F. and Viret, J. (1993). Fluidity of chicken ventricular plasma membranes during development in-ovo and after birth: spin labelling and fluorescence studies. *J. Mol. Cell. Cardiol.* **25**, 1439-1444.

Dixon, J. M. and Loretz, C. A. (1986). Luminal alkalinization in the intestine of the goby. *J. Comp. Physiol. B* **156**, 803-811.

Faelli, A., Tosco, M., Orsenigo, M. N. and Esposito, G. (1984). Effects of the stilbene derivatives SITS and DIDS on intestinal ATPase activities. *Pharmacol. Res. Commun.* **16**, 339-350.

Garcia-Romeu, F., Cossins, A. R. and Motais, R. (1991). Cell volume regulation by trout erythrocytes: characteristics of the transport systems activated by hypotonic swelling. *J. Physiol.* **440**, 547-567.

Garçon, D. P., Masui, D. C., Mantelatto, F. L., McNamara, J. C., Furriel, R. P. and Leone, F. A. (2007). K^+ and NH_4^+ modulate gill (Na^+, K^+)-ATPase activity in the blue crab, *Callinectes ornatus*: fine tuning of ammonia excretion. *Comp. Biochem. Physiol.* **147A**, 145-155.

Genz, J., Esbaugh, A. J. and Grosell, M. (2011). Intestinal transport following transfer to increased salinity in an anadromous fish (*Oncorhynchus mykiss*). *Comp. Biochem. Physiol.* **159A**, 150-158.

Gonçalves, A. F., Castro, L. F. C., Pereira-Wilson, C., Coimbra, J. and Wilson, J. M. (2007). Is there a compromise between nutrient uptake and gas exchange in the gut of *Misgurnus anguillicaudatus*, an intestinal air-breathing fish? *Comp. Biochem. Physiol.* **2D**, 345-355.

Graham, J. B. (1997). *Air-Breathing Fishes: Evolution, Diversity and Adaptation.* San Diego, CA: Academic Press.

Grosell, M. (2006). Intestinal anion exchange in marine fish osmoregulation. *J. Exp. Biol.* **209**, 2813-2827.

Grosell, M. (2007). Intestinal transport processes in marine fish osmoregulation. In *Fish Osmoregulation* (ed. B. Baldisserotto, J. M. Mancera and B. G. Kapoor), pp. 333-358. Enfield, NH: Science Publishers.
Grosell, M. (2010). The role of the gastrointestinal tract in salt and water balanace. In *The Multifunctional Gut of Fish*, Vol. 30 (ed. M. Grosell, A. P. Farrell and C. J. Brauner,), pp. 135-164. London, UK: Academic Press.
Grosell, M. and Genz, J. (2006). Ouabain-sensitive bicarbonate secretion and acid absorption by the marine teleost fish intestine play a role in osmoregulation. *Am. J. Physiol.* **291**, R1145-R1156.
Grosell, M. and Jensen, F. B. (1999). NO_2^- uptake and HCO_3^- excretion in the intestine of the European flounder (*Platichthys flesus*). *J. Exp. Biol.* **202**, 2103-2110.
Grosell, M., Laliberte, C. N., Wood, S., Jensen, F. B. and Wood, C. M. (2001). Intestinal HCO_3^- secretion in marine teleost fish: evidence for an apical rather than a basolateral Cl^-/HCO_3^- exchanger. *Fish Physiol. Biochem.* **24**, 81-95.
Grosell, M., Gilmour, K. M. and Perry, S. F. (2007). Intestinal carbonic anhydrase, bicarbonate, and proton carriers play a role in the acclimation of rainbow trout to seawater. *Am. J. Physiol.* **293**, R2099-R2111.
Grosell, M., Genz, J., Taylor, J. R., Perry, S. F. and Gilmour, K. M. (2009a). The involvement of H^+-ATPase and carbonic anhydrase in intestinal HCO_3^- secretion in seawater-acclimated rainbow trout. *J. Exp. Biol.* **212**, 1940-1948.
Grosell, M., Mager, E. M., Williams, C. and Taylor, J. R. (2009b). High rates of HCO_3^- secretion and Cl^- absorption against adverse gradients in the marine teleost intestine: the involvement of an electrogenic anion exchanger and H^+-pump metabolon? *J. Exp. Biol.* **212**, 1684-1696.
Ip, Y. K., Randall, D. J., Kok, T. K. T., Barzaghi, C., Wright, P. A., Ballantyne, J. S., Wilson, J. M. and Chew, S. F. (2004). The giant mudskipper *Periophthalmodon schlosseri* facilitates active NH_4^+ excretion by increasing acid excretion and decreasing NH_3 permeability in the skin. *J. Exp. Biol.* **207**, 787-801.
Jeuken, M. (1957). A study of the respiration of *Misgurnus fossilis* (L.) the pond loach. PhD dissertation, University of Leiden, Germany.
Katynski, A. L., Vijayan, M. M., Kennedy, S. W. and Moon, T. W. (2004). 3,3′,4,4′,5-Pentachlorobiphenyl (PCB 126) impacts hepatic lipid peroxidation, membrane fluidity and beta-adrenoceptor kinetics in chick embryos. *Comp. Biochem. Physiol.* **137C**, 81-93.
Kikeri, D., Sun, A., Zeidel, M. L. and Hebert, S. C. (1989). Cell membranes impermeable to NH_3. *Nature* **339**, 478-480.
Kleyman, T. R. and Cragoe, E. J., Jr (1988). Amiloride and its analogs as tools in the study of ion transport. *J. Membr. Biol.* **105**, 1-21.
Knepper, M. A., Packer, R. and Good, D. W. (1989). Ammonium transport in the kidney. *Physiol. Rev.* **69**, 179-249.
Kumai, Y. and Perry, S. F. (2011). Ammonia excretion via Rhcg1 facilitates Na uptake in larval zebrafish, *Danio rerio*, in acidic water. *Am. J. Physiol.* **301**, R1517-R1528.
Kurita, Y., Nakada, T., Kato, A., Doi, H., Mistry, A. C., Chang, M.-H., Romero, M. F. and Hirose, S. (2008). Identification of intestinal bicarbonate transporters involved in formation of carbonate precipitates to stimulate water absorption in marine teleost fish. *Am. J. Physiol.* **294**, R1402-R1412.
Lande, M. B., Donovan, J. M. and Zeidel, M. L. (1995). The relationship between membrane fluidity and permeabilities to water, solutes, ammonia, and protons. *J. Gen. Physiol.* **106**, 67-84.
Lee, S., Lee, H. J., Yang, H. S., Thornell, I. M., Bevensee, M. O. and Choi, I. (2010). Sodium-bicarbonate cotransporter NBCn1 in the kidney medullary thick ascending limb cell line is upregulated under acidic conditions and enhances ammonium transport. *Exp. Physiol.* **95**, 926-937.
Lin, H. and Randall, D. (1991). Evidence for the presence of an electrogenic proton pump on the trout gill epithelium. *J. Exp. Biol.* **161**, 119-134.
Mallery, C. H. (1983). A carrier enzyme basis for ammnium excretion in teleost gill. NH_4^+-stimulated Na-dependent ATPase activity in *Opsanus beta*. *Comp. Biochem. Physiol.* **74A**, 889-897.
Maren, T. H. (1977). Use of inhibitors in physiological studies of carbonic anhydrase. *Am. J. Physiol.* **232**, F291-F297.
Marshall, W. S. and Grosell, M. (2006). Ion transport and osmoregulation in fish. In *The Physiology of Fishes* (ed. D. H. Evans and J. B. Claiborne), pp. 177-230. Boca Raton, FL: CRC Press.
McDonald, M. D. and Grosell, M. (2006). Maintaining osmotic balance with an aglomerular kidney. *Comp. Biochem. Physiol.* **143A**, 447-458.
McMahon, B. R. and Burggren, W. W. (1987). Respiratory physiology of intestinal air breathing in the teleost fish *Misgurnus anguillicaudatus*. *J. Exp. Biol.* **133**, 371-393.
Moreira-Silva, J., Tsui, T. K., Coimbra, J., Vijayan, M. M., Ip, Y. K. and Wilson, J. M. (2010). Branchial ammonia excretion in the Asian weatherloach *Misgurnus anguillicaudatus*. *Comp. Biochem. Physiol.* **151C**, 40-50.
Randall, D. J., Wilson, J. M., Peng, K. W., Kok, T. W., Kuah, S. S. L., Chew, S. F., Lam, T. J. and Ip, Y. K. (1999). The mudskipper, *Periophthalmodon schlosseri*, actively transports NH_4^+ against a concentration gradient. *Am. J. Physiol.* **277**, R1562-R1567.
Shih, T. H., Horng, J. L., Hwang, P. P. and Lin, L. Y. (2008). Ammonia excretion by the skin of zebrafish (*Danio rerio*) larvae. *Am. J. Physiol.* **295**, C1625-C1632.
Shih, T. H., Horng, J. L., Liu, S. T., Hwang, P. P. and Lin, L. Y. (2012). Rhcg1 and NHE3b are involved in ammonium-dependent sodium uptake by zebrafish larvae acclimated to low-sodium water. *Am. J. Physiol.* **302**, R84-R93.
Silva, P., Solomon, R., Spokes, K. and Epstein, F. H. (1977). Ouabain inhibition of gill Na-K-ATPase: relationship to active chloride transport. *J. Exp. Zool.* **199**, 419-426.
Singh, S. K., Binder, H. J., Geibel, J. P. and Boron, W. F. (1995). An apical permeability barrier to NH_3/NH_4^+ in isolated, perfused colonic crypts. *Proc. Natl. Acad. Sci. USA* **92**, 11573-11577.
Smith, P. K., Krohn, R. I., Hermanson, G. T., Mallia, A. K., Gartner, F. H., Provenzano, M. D., Fujimoto, E. K., Goeke, N. M., Olson, B. J. and Klenk, D. C. (1985). Measurement of protein using bicinchoninic acid. *Anal. Biochem.* **150**, 76-85.
Taylor, J. R., Cooper, C. A. and Mommsen, T. P. (2011). Implications of GI function for gas exchange, acid-base balance and nitrogen metabolism. In *The Multifunctional Gut of Fish*, Vol. 30 (ed. M. Grosell, A. P. Farrell and C. J. Brauner), pp. 213-259. London, UK: Academic Press.
Tokuda, S., Shimamoto, C., Yoshida, H., Murao, H., Kishima, G. I., Ito, S., Kubota, T., Hanafusa, T., Sugimoto, T., Niisato, N. et al. (2007). HCO_3^--dependent pH(i) recovery and over acidification induced by NH_4^+ pulse in rat lung alveolar type II cells: HCO_3^--dependent NH_3 excretion from lungs? *Pflugers Arch.* **455**, 223-239.
Tsui, T. K. N., Randall, D. J., Chew, S. F., Jin, Y., Wilson, J. M. and Ip, Y. K. (2002). Accumulation of ammonia in the body and NH_3 volatilization from alkaline regions of the body surface during ammonia loading and exposure to air in the weather loach *Misgurnus anguillicaudatus*. *J. Exp. Biol.* **205**, 651-659.
Verdouw, H., van Echeld, C. J. A. and Dekkers, E. M. J. (1978). Ammonia determination based on indophenol formation with sodium salicylate. *Water Res.* **12**, 399-402.
Weihrauch, D., Wilkie, M. P. and Walsh, P. J. (2009). Ammonia and urea transporters in gills of fish and aquatic crustaceans. *J. Exp. Biol.* **212**, 1716-1730.
Weiner, I. D. and Verlander, J. W. (2011). Role of NH_3 and NH_4^+ transporters in renal acid-base transport. *Am. J. Physiol. Renal Physiol.* **300**, F11-F23.
Wilson, J. M. and Castro, L. F. C. (2011). Morphological diversity of the gastrointestinal tract in fishes. In *The Multifunctional Gut of Fish*, Vol. 30 (ed. M. Grosell, A. P. Farrell and C. J. Brauner), pp. 1-55. London, UK: Academic Press.
Wilson, R. W., Wright, P. M., Munger, S. and Wood, C. M. (1994). Ammonia excretion in freshwater rainbow trout (*Oncorhynchus mykiss*) and the importance of gill boundary layer acidification: lack of evidence for Na^+/NH_4^+ exchange. *J. Exp. Biol.* **191**, 37-58.
Wilson, R. W., Gilmour, K. M., Henry, R. P. and Wood, C. M. (1996). Intestinal base excretion in the seawater-adapted rainbow trout: a role in acid-base balance? *J. Exp. Biol.* **199**, 2331-2343.
Wolf, K. (1963). Physiological salines for fresh-water teleosts. *Progr. Fish-Cult.* **25**, 135-140.
Wright, P. A. and Wood, C. M. (2009). A new paradigm for ammonia excretion in aquatic animals: role of Rhesus (Rh) glycoproteins. *J. Exp. Biol.* **212**, 2303-2312.
Wu, S. C., Horng, J. L., Liu, S. T., Hwang, P. P., Wen, Z. H., Lin, C. S. and Lin, L. Y. (2010). Ammonium-dependent sodium uptake in mitochondrion-rich cells of medaka (*Oryzias latipes*) larvae. *Am. J. Physiol.* **298**, C237-C250.
Zachos, N. C., Tse, M. and Donowitz, M. (2005). Molecular physiology of intestinal Na^+/H^+ exchange. *Annu. Rev. Physiol.* **67**, 411-443.

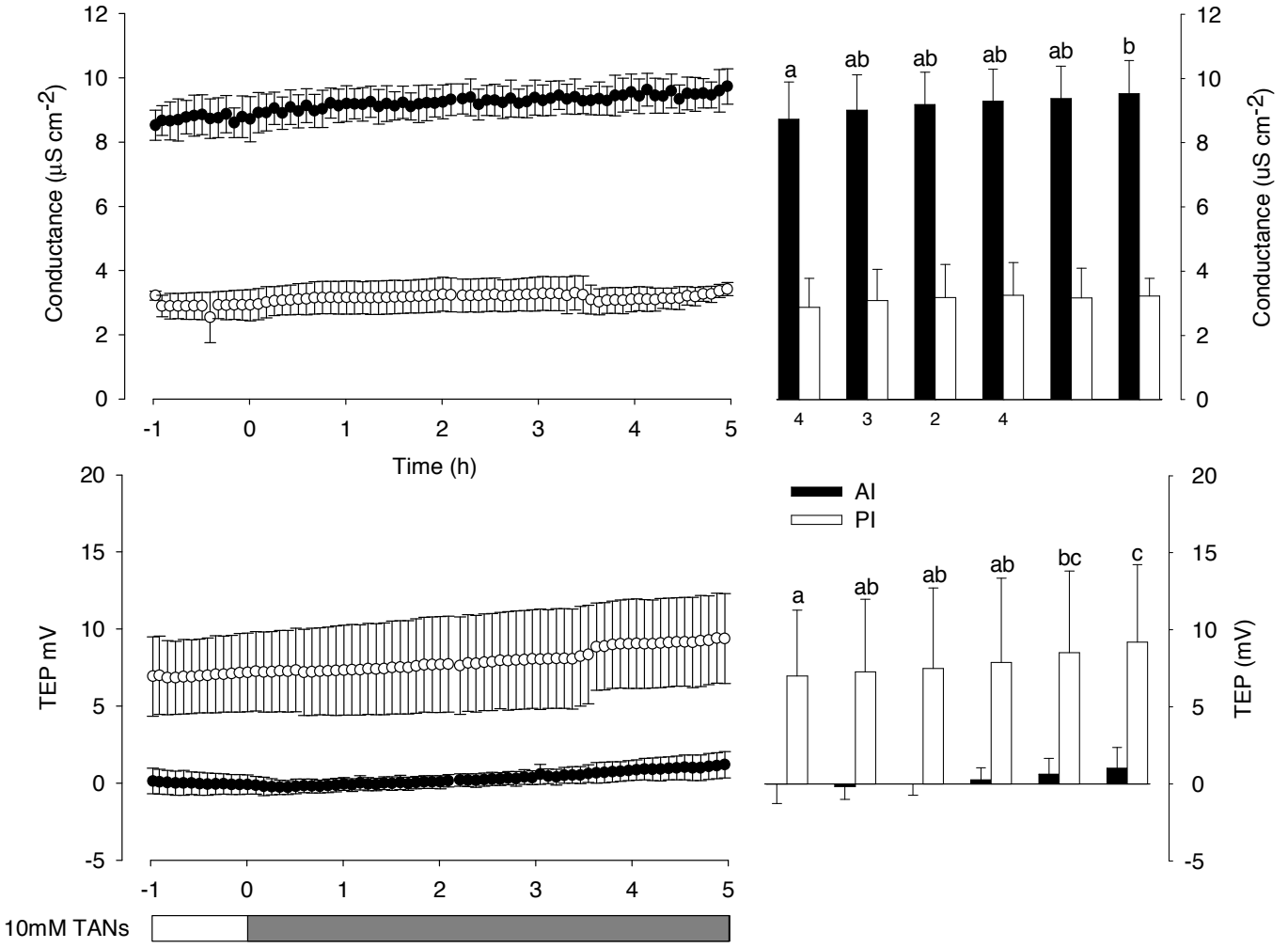

Fig. S1. Conductance (G, µSi cm^{-2}) and transepithelial potential (TEP, mV) of the weatherloach anterior (black) and posterior (white) intestine under control (Pre-TAN) and ammonia (10 mmol l^{-1} TAN serosal) exposure conditions. (A) G and (B) TEP measurements made over 5 min intervals. (C,D) The same data (respectively) averaged over hour periods. Bars with like characters are not significantly different (N=4).

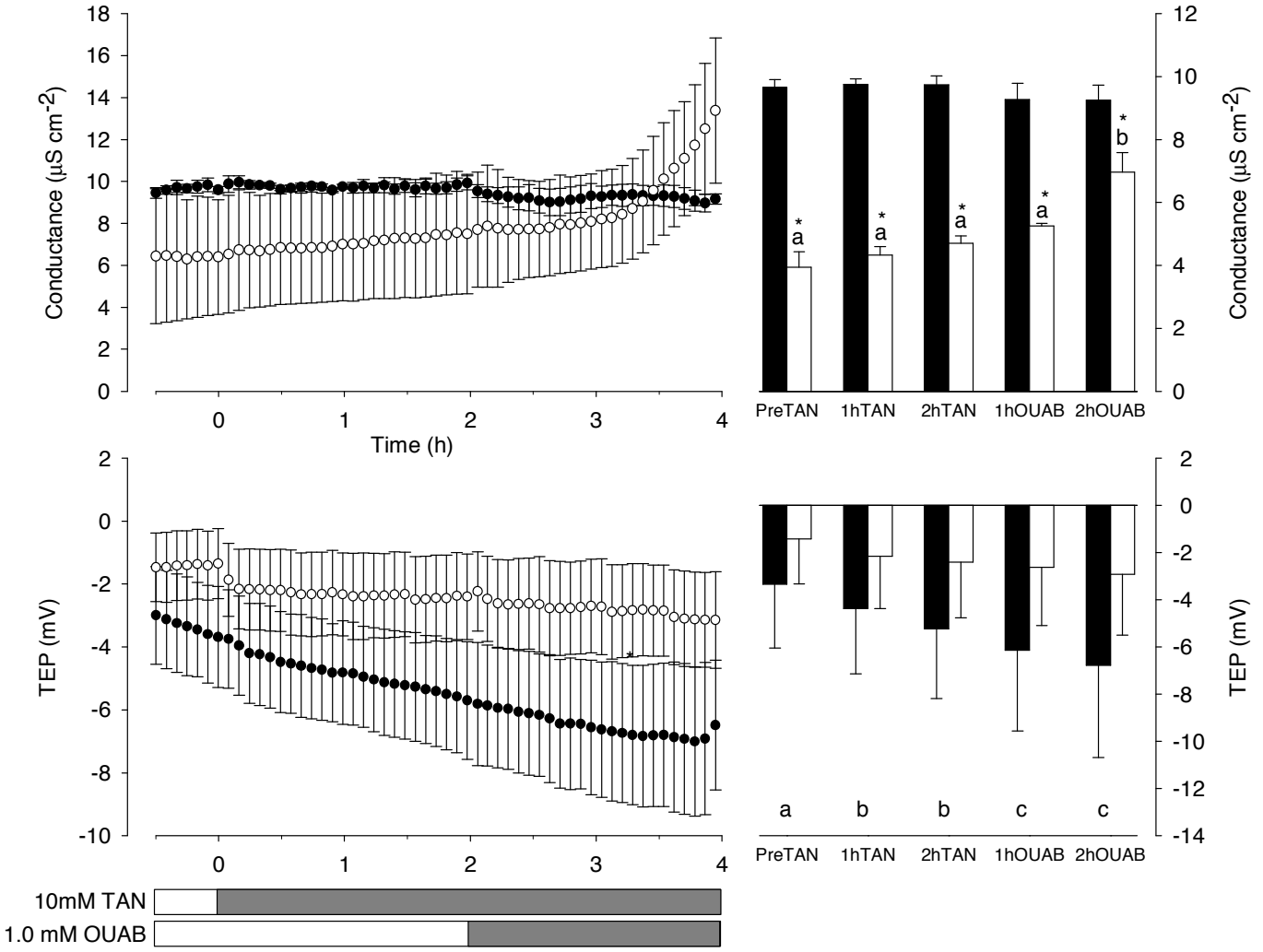

Fig. S2. Conductance (G, µSi cm^{-2}) and transepithelial potential (TEP, mV) of the weatherloach anterior (black) and posterior (white) intestine under control (Pre-TAN) and ammonia (10 mmol l^{-1} TAN serosal) exposure conditions followed by serosal 1 mmol l^{-1} ouabain treatment. (A) G and (B) TEP measurements made over 5 min intervals. (C,D) The same data (respectively) averaged over hour periods. Bars with like characters are not significantly different (N=3).

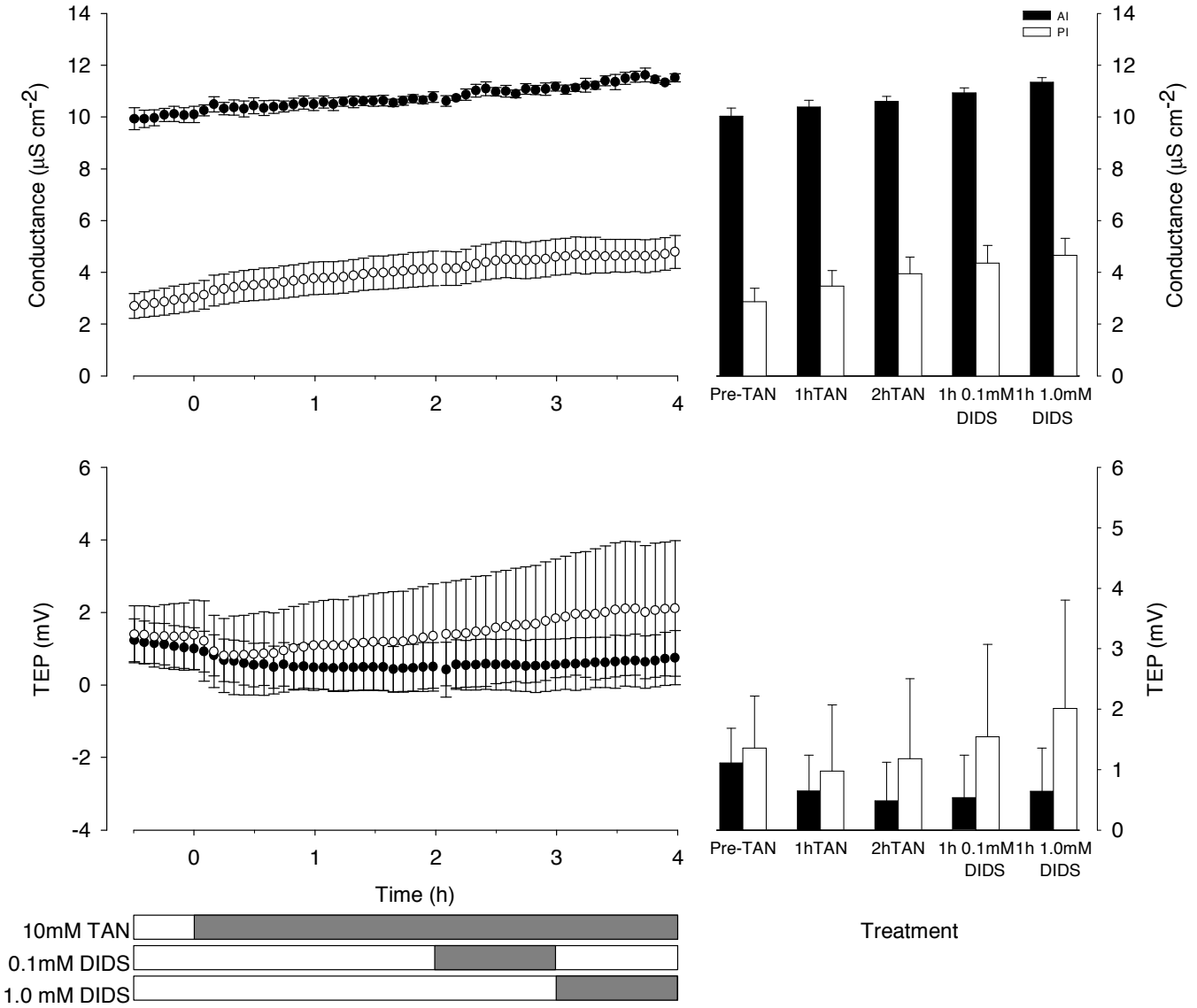

Fig. S3. Conductance (G, µSi cm^{-2}) and transepithelial potential (TEP, mV) of the weatherloach anterior (black) and posterior (white) intestine under control (Pre-TAN) and ammonia (10 mmol l^{-1} TAN serosal) exposure conditions followed by mucosal 0.1 and 1 mmol l^{-1} DIDS treatment. (A) G and (B) TEP measurements made over 5 min intervals. (C,D) The same data (respectively) averaged over hour periods. Bars with like characters are not significantly different (N=4).

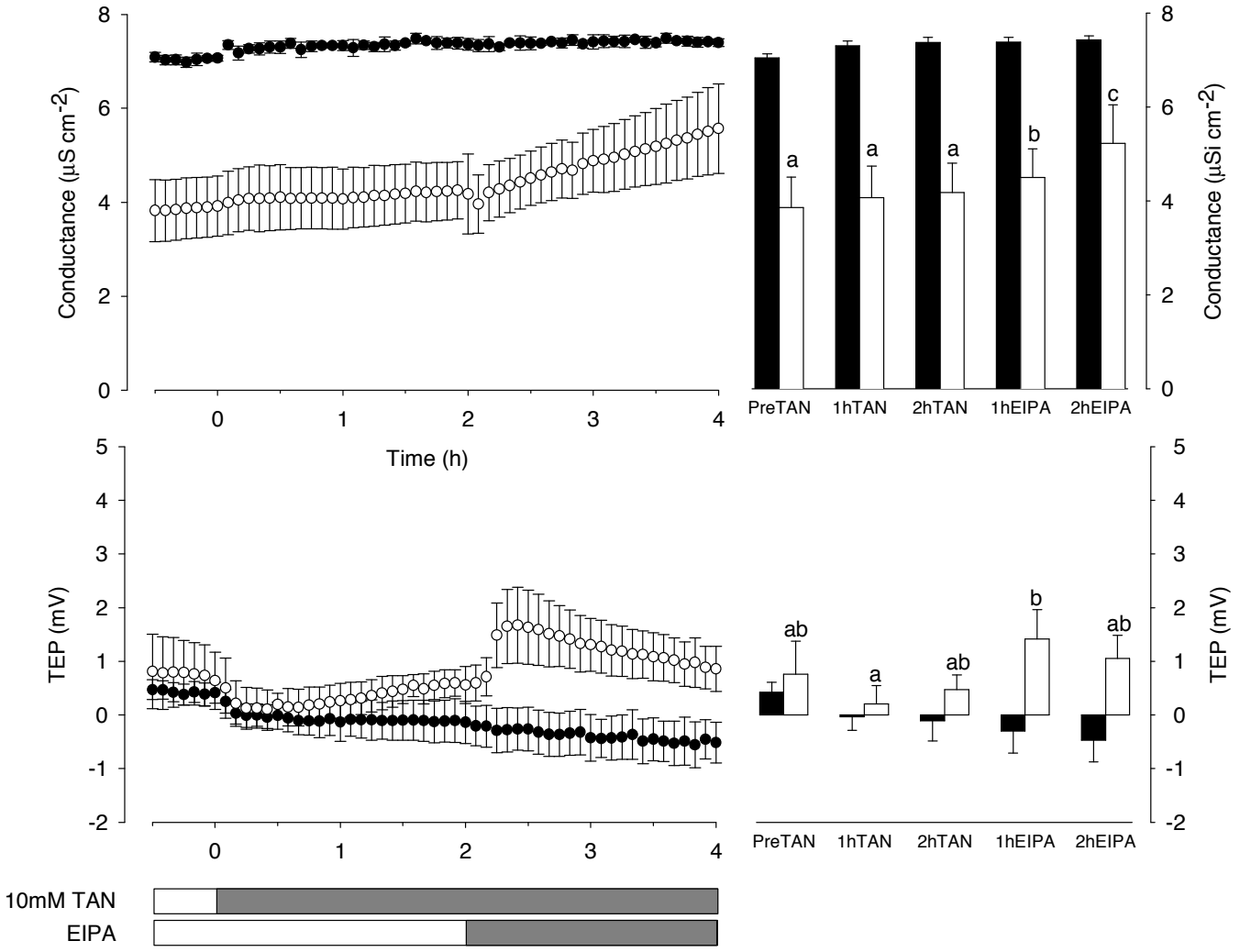

Fig. S4. Conductance (G, µSi cm^{-2}) and transepithelial potential (TEP, mV) of the weatherloach anterior (black) and posterior (white) intestine under control (Pre-TAN) and ammonia (10 mmol l^{-1} TAN serosal) exposure conditions followed by mucosal 1 mmol l^{-1} EIPA treatment. (A) G and (B) TEP measurements made over 5 min intervals. (C,D) The same data (respectively) averaged over hour periods. Bars with like characters are not significantly different (N=4).

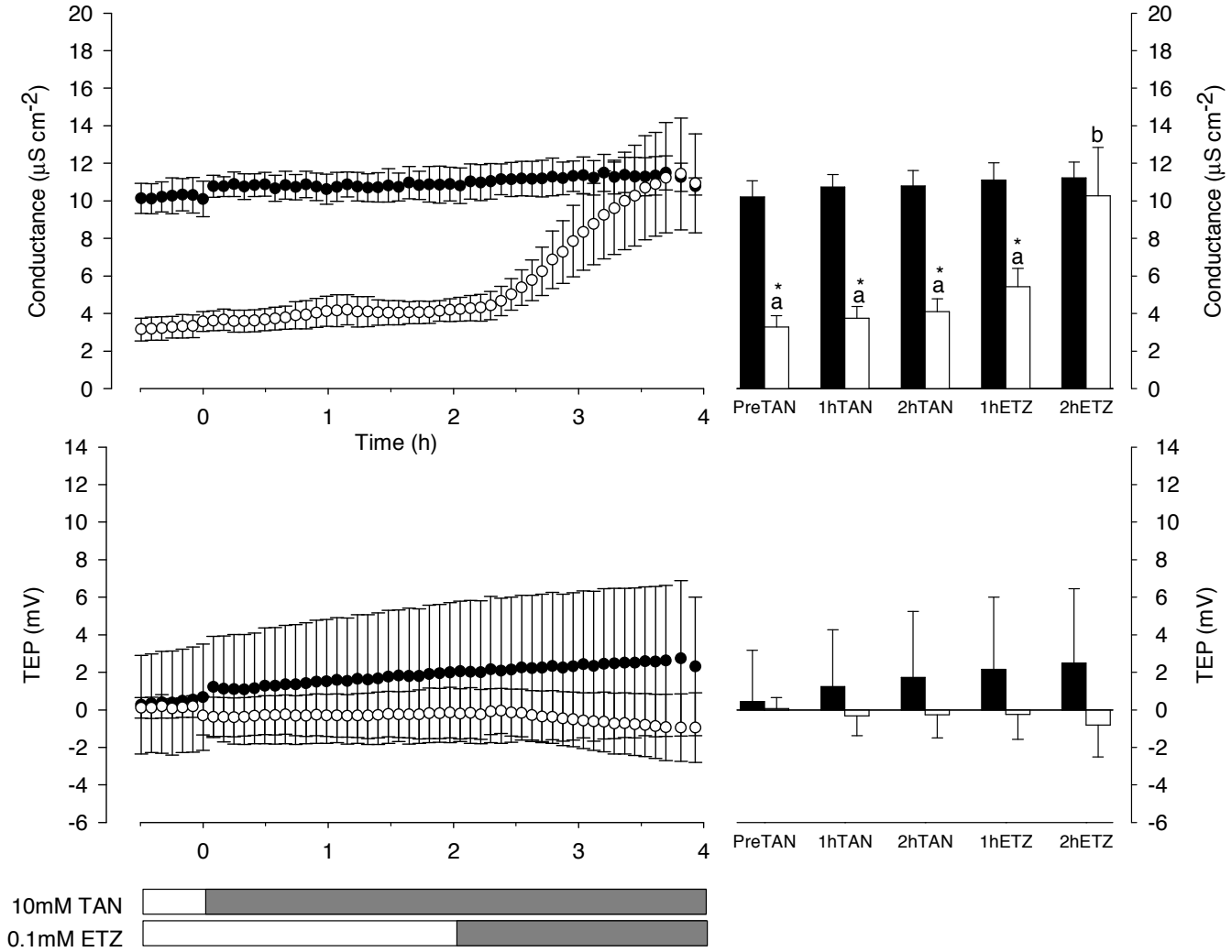

Fig. S5. Conductance (G, μSi cm^{-2}) and transepithelial potential (TEP, mV) of the weatherloach anterior (black) and posterior (white) intestine under control (Pre-TAN) and ammonia (10 mmol l^{-1} TAN serosal) exposure conditions followed by 1 mmol l^{-1} ETZ treatment. (A) G and (B) TEP measurements made over 5 min intervals. (C,D) The same data (respectively) averaged over hour periods. Bars with like characters are not significantly different (N=4).

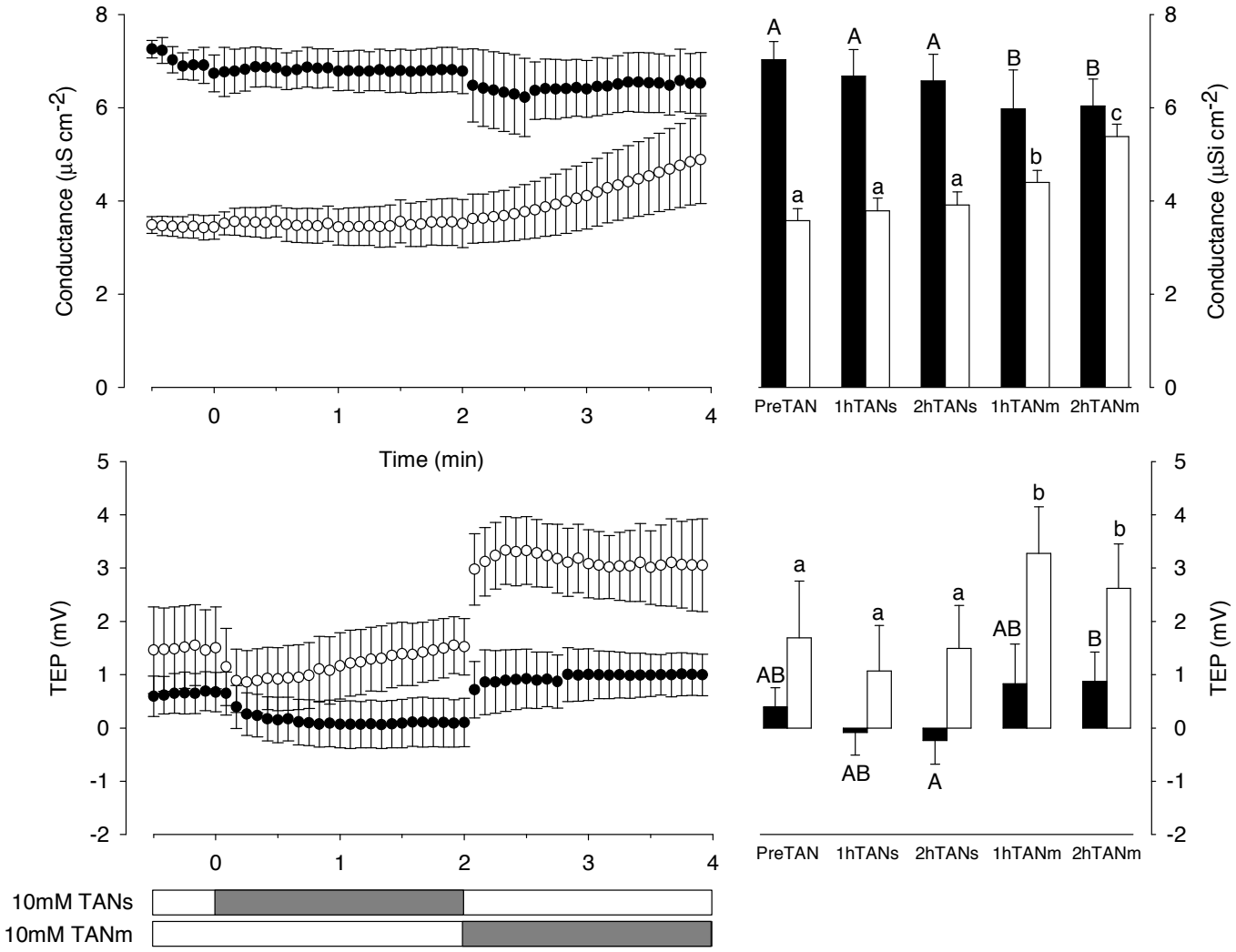

Fig. S6. Conductance (G, μSi cm^{-2}) and transepithelial potential (TEP, mV) of the weatherloach anterior (black) and posterior (white) intestine under control (Pre-TAN) and serosal–mucosal (10 mmol l^{-1} TAN serosal) and mucosal–serosal (10 mmol l^{-1} TAN mucosal) ammonia gradient conditions. (A) G and (B) TEP measurements made over 5 minute intervals. (C,D) The same data (respectively) averaged over hour periods. Bars with like characters are not significantly different (N=4).